Special Issue on "Theoretical and Computational Chemistry"

J. Indian Chem. Soc.,
Vol. 96, July 2019, pp. 1003-1009

A new model system preparation approach for ONIOM: Accurate estimation of energies and forces of molecules with π-bonds

Srinivasarao Mande and K. V. Jovan Jose*

School of Chemistry, University of Hyderabad, Hyderabad-500 046, Telangana, India

E-mail: jovanjose@uohyd.ac.in

Manuscript received online 13 May 2019, revised and accepted 29 May 2019

We propose a general procedure to treat the model system boundary region within the ONIOM framework involving covalent double bonds. The basis of the treatment is to saturate the two-dangling valences of the covalently double bonded support-atom with two hydrogen atoms to perform separate ONIOM calculations. We have developed a systematic procedure to project back the link-atom force components onto the host- and support-atoms of the real system. We have benchmarked our ONIOM model by evaluating the dissociation energies and atomic forces of 10 molecules with isolated and conjugated double bonds. ONIOM reaction energy shows a fair agreement with the full calculation (FC) at high-level, and the typical errors in reaction energies are within 1 kcal/mol. For benchmarking the accuracy of the forces, we have performed the geometry optimization, and the geometrical parameters show a fair agreement with the FC. The agreement of the ONIOM results with the FC shows that the adopted procedure is a pragmatic method to construct the model system for systems involving double bonds at the boundary region. The proposed procedure to treat link-atom is economical and adaptable within any fragment-based methods involving the construction of model systems, for the accurate estimation of energies and forces of large molecules.

Keywords: ONIOM method, *ab initio* calculations, Hartree-Fock (HF) theory, Density Functional Theory (DFT), large molecules.

Introduction

Theoretical treatment of large molecules has gained extensive attention in the last three decades[1–4]. However, the high scaling of accurate *ab initio* computational methods with system size limited their applications for large molecules[5–10]. The hybrid energy methods have facilitated to balance the accuracy with the scaling of computational methods[11–18]. Hybrid energy QM/QM methods treat the chemically important region of the large molecule (Region I) at a high level of theory and the environment, the rest of the molecule (Region II) at a low level of theory. ONIOM approach of Morokuma and co-workers is the most widely used QM/QM hybrid embedding scheme[19–25]. A two-layer ONIOM hybrid energy is evaluated from three separate well-defined calculations of the entire system (I+II, Low) and Region I (High, Low). In the standard notation used in ONIOM, the extrapolated total energy expression is written as

$$E^{\text{total}} = E_{\text{RL}}(\text{I+II}) - E_{\text{ML}}(\text{I}) + E_{\text{MH}}(\text{I}) \quad (1)$$

where R stands for the "real system" (Regions I + II), M stands for the "model system" (Region I), and the High (H) and Low (L) refers to the levels of theory. The hybrid-energy expression defined in eq. (1) allows one to couple different computational chemistry methods for which energies and gradients are available.

In covalently single-bonded systems, the model system is constructed from Region I by saturating the "dangling bonds" with the addition of link H-atoms. The electronic coupling between the Regions I and II are accounted only at the low level of theory, in the E_{RL} calculation. Truncation of Region I with a capping H-atom is a possible source of error in the ONIOM extrapolation method. The resulting charge imbalance can impose limitations on the performance of the ONIOM method. The accuracy of the ONIOM model profoundly depends on the treatment of the link atom. There are special methods in the literature to treat the charge-transfer at the Region I and II boundary by the methods of balancing chemical potentials[26–29], Mulliken charges (ONIOM-CT)[30] and electrostatic potential (ESP-ONIOM-CT) in the model system boundary[31–33].

The general procedure followed in fragment-based meth-

ods is to scissor only the weakly interacting or covalent single bonds. The double bonds and higher aromatic rings are kept intact in the model system construction procedure. Gadre *et al.* have come up with a way to saturate the dangling valency of conjugated double bonds[34]. However, the charge transfer at the boundaries may be higher when we construct a model system by cutting double bonds. Also, while scissoring an isolated covalent doubles-bond, a single H-link-atom can't account for all the dangling valances of the host-atom in the model system. In the current scenario, there is no method devised to scissor an isolated covalently bonded double-bond model system to calculate the energy and atomic forces. In the present work, we have come up a general procedure to scissor double-bonds in the model-system preparation stage, perform the separate model-system calculations (Low and High) and project-back the energy gradient components on to the real system host- and supporting-atoms. In the present work, some of the questions that we attempt to address are:

(1) Can we develop a general procedure to scissor a covalent double-bond, while constructing the model system in the ONIOM method?

(2) Can the 'two-link-atom' ONIOM model reproduce the reaction energies compared to FC at high-level of theory?

(3) Can we develop a general procedure to project-back the two-link atom force components on to the real system while performing a ONIOM geometry optimization?

(4) How would be the agreement of the 'two-link-atom' ONIOM optimized geometry in comparison to FC at high-level of theory?

Considering all these questions, we have come up with a general procedure to treat the ONIOM model system boundary region (between Region I and II) involving covalent double bond. The following section discusses the general procedure to construct model systems with double-bonds, and the next section presents a benchmark of the method.

Methods

This section describes the theory for the treatment of link-atom along with the covalent double bond. In our work, we have developed a method to treat the boundary between Region I and II in ONIOM model. This is accomplished via a novel "two-link-atom ONIOM model system preparation" step. In our initial implementation, we treat the link atoms on the model system as an electron buffer region and saturate the dangling valency of the model system by two-link atoms. The methodology for a three- or higher-layer ONIOM method is the same and will not be discussed explicitly.

The atoms common to the model system (Region I) and real system (Region I and II) is noted as $\boldsymbol{R}_1$. Atoms of the host-atom in the Region II is denoted as $\boldsymbol{R}_3$, and all atoms in the Region II, other than the host-atom is denoted as $\boldsymbol{R}_4$. The coordinates of the link atoms, that replaces the host-atom of the Region II is denoted as $\boldsymbol{R}_2$. The model system is constructed from the coordinates, $\boldsymbol{R}_1$ and $\boldsymbol{R}_2$. The link atom coordinate ($\boldsymbol{R}_2$) is placed to mimic the moment of the support ($\boldsymbol{R}_1$) and host ($\boldsymbol{R}_3$) atoms, as depicted in Fig. 1(A). Therefore, we can say that the $\boldsymbol{R}_2 = f(\boldsymbol{R}_1, \boldsymbol{R}_3)$. We saturate the valences of a double bond support atom ($\boldsymbol{R}_1$) with two-link H-atoms (denoted as $\boldsymbol{R}_2^{l1}$ and $\boldsymbol{R}_2^{l2}$). The link H-atom coordinate positioned relative to the support- and host-atom coordinates through the following relationship.

$$\boldsymbol{r}_2^{l1} = [r_1 + g(\boldsymbol{r}_3 - \boldsymbol{r}_1)]\, R(\theta) \quad (2)$$

$$\boldsymbol{r}_2^{l2} = [\boldsymbol{r}_1 + g(\boldsymbol{r}_3 - \boldsymbol{r}_1)]\, R(-\theta) \quad (3)$$

Here, g is the scale factor or a distance parameter is defined as the ratio of covalent bond lengths of Host-to-Link to that of Host-to-Support atoms, it hold the same meaning as defined in the standard implementation earlier by Dapprich *et al.*[35]. For example, the magnitude of the g is defined as the ratio of covalent C-H bond length (1.084 Å) divided by the C=C bond length (1.339 Å). The g-value comes to be a constant, 0.899 Å, but the coordinates of the link-atom are not a constant in the optimization cycles. In this work, we have considered only cutting the C=C double bonds. The $R(\theta)$ and $R(-\theta)$ are the rotational matrices to rotate the link-hydrogen atom in clockwise and anti-clockwise directions, after placing the link-hydrogen atom at a scaled distance from Host- and Support-atoms. We apply the same angle of rotation but in the clockwise and anti-clockwise directions for each link-atom to get the final coordinates, $\boldsymbol{r}_2^{l1}$ and $\boldsymbol{r}_2^{l2}$. Also, we assume that the rotation matrix is a constant and is independent of the extension or contraction of Host-Support bond lengths in the optimization cycles. Fig. 1 depicts the stages of the model system preparation in the ONIOM calculation.

(1) For finding the coordinates of the two-link H-atoms, virtual-link atoms (in grey color) as depicted in Fig. 1(A) is placed at a scaled distance, along the direction of the bond connecting support- and host-atoms. The coordinates of the virtual-link H-atom is constructed from the first part of the eqs. (2) and (3), as depicted in Fig. 1(A).

(2) The coordinates of the first link atom, $\boldsymbol{r}_2^{l1}$ is obtained by rotating the virtual-link atom (in grey color) in Fig. 1(A) through a rotation matrix, $R(\theta)$ by an angle θ. The second link atom coordinate, $\boldsymbol{r}_2^{l2}$ is obtained by an anti-clockwise rotation of the virtual-link H-atom, by an angle $-\theta$.

(3) Perform the independent calculations on the model system at high- and low-levels of theory.

(4) The ONIOM hybrid energy is constructed from the independent real-low (E_{rl}), model-low (E_{ml}), and model-high (E_{mh}) energies, through the general expression as defined in eq. (1).

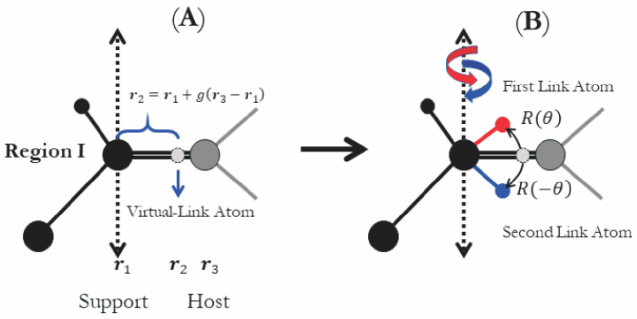

Fig. 1. Cartoon showing the two-link atom ONIOM model system preparation step by scissoring a covalent double bond. (A) A virtual-link atom (grey color) is placed at a scaled distance from the host- and support-atoms. (B) The virtual-link atom (grey color) atom coordinates are rotated in clockwise and anti-clockwise to get the coordinates of the link atoms.

(5) The atomic force evaluation, first link-atom ($\boldsymbol{R}_2^{l1}$) force components are rotated-back on to the virtual-link atom (grey color) using the same rotation matrix as in eq. (2), but in opposite direction, as depicted in Fig. 1(B). Then the virtual-link atom force components are projected back onto the supporting- and host-atoms through a general Jacobian projection method. These two-steps are incorporated in the second and third terms in eq. (4). A similar procedure is followed for the second link atom ($\boldsymbol{R}_2^{l2}$) as well, and it result in fourth and fifth terms in eq. (4).

$$F_a = \frac{\partial E_{total}}{\partial X_a} = \frac{\partial E_{rl}}{\partial X_a} - \left(\frac{\partial E_{ml}}{\partial X_a^{l1}}\right) \boldsymbol{J}(\boldsymbol{R}_2^{l1}; \boldsymbol{R}_1, \boldsymbol{R}_3) R(\theta) + \left(\frac{\partial E_{mh}}{\partial X_a^{l1}}\right) \boldsymbol{J}(\boldsymbol{R}_2^{l1}; \boldsymbol{R}_1, \boldsymbol{R}_3) R(\theta) - \left(\frac{\partial E_{ml}}{\partial X_a^{l2}}\right) \boldsymbol{J}(\boldsymbol{R}_2^{l2}; \boldsymbol{R}_1, \boldsymbol{R}_3) R(-\theta) + \left(\frac{\partial E_{mh}}{\partial X_a^{l2}}\right) \boldsymbol{J}(\boldsymbol{R}_2^{l2}; \boldsymbol{R}_1, \boldsymbol{R}_3) R(-\theta) \quad (4)$$

Here, the index *a* corresponds to the Cartesian components of X, Y or Z directions. The elements of the 3×3 Jacobi matrix ($\boldsymbol{J}$) to project the link-atom Cartesian component onto the corresponding supporting-atom component is defined as the partial derivative of the Cartesian component of the former with respect to the latter,

$$\frac{dr_{2,a}}{dr_{1,b}} = (1 - g)\delta_{a,b} \quad (5)$$

Here, $\delta_{a,b}$ is the Kronecker delta, and *a* and *b* are the Cartesian components. Similarly, an analogous partial derivative with respect to the host-atom defines the Jacobi matrix element for projecting the link-atom forces onto the host-atom,

$$\frac{dr_{2,a}}{dr_{3,b}} = (g)\delta_{a,b} \quad (6)$$

Thus, the force vector elements of the host- and support-atoms are modified from the link-atom Jacobi projection method.

(6) These atomic energies and forces are fed back to the Gaussian G09 for performing the geometry optimization cycles[36]. Steps 1 to 4 is followed to construct the extrapolated energy, gradients to perform the optimization cycles and is carried out till convergence.

The steps mentioned above are coded in a Fortran language and interfaced with Gaussian 09 suite of packages. For benchmarking our method, we have considered a set of

molecules depicted in Fig. 2. To have a fresh look at the electron delocalization and charge transfer at the boundary region, we thought that it would be worthwhile to consider molecules involving isolated and conjugated double bonds. All the geometry optimization is performed at B3LYP/6-31G using the Gaussian suite of packages[36]. For calculating the reaction energy, the single point energy is calculated on these molecules at B3LYP/6-311+G(d,p) level of theory, and the ONIOM calculation is performed at B3LYP/6-311+G(d,p): HF/6-31g(d) levels of theory.

Results and discussion

(1) Deprotonation energies of molecules

For benchmarking our approach within ONIOM model, we have considered a set of conjugated and isolated covalently bonded molecules depicted in Fig. 2. Each of the molecules is associated with an organic functional group, and we have evaluated the deprotonation energies of the functional group protons at FC at B3LYP/6-311+G(d,p) and ONIOM at (B3LYP/6-311+G(d,p): HF/6-31G(d)) levels of theory. We constructed the model system around the organic functional group with a similar number of atoms in all the conjugated and isolated double bonded molecules.

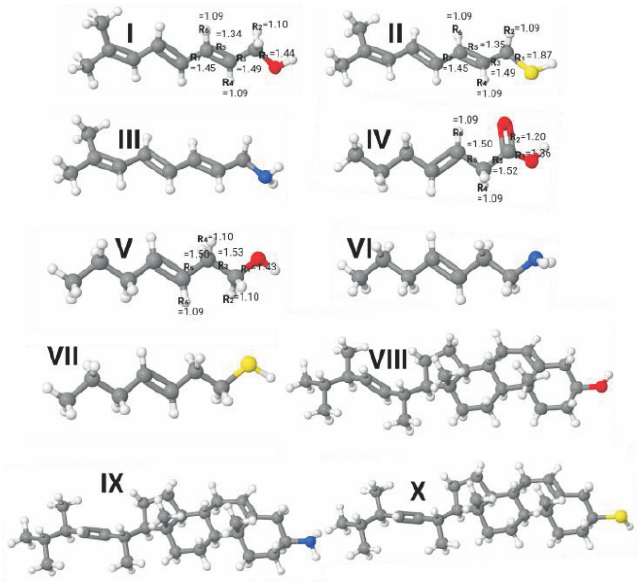

Fig. 2. Depict the benchmark molecules employed for the two-link-atom ONIOM model. The geometrical parameters compared in Table 2 are depicted {*Ri*} for each of the molecules. In each benchmark system, the right-hand side of the molecule is the model system. The middle covalent bond is scissored in all the molecules while constructing the two-link-atom ONIOM model system preparation.

For performing this comparison, we have optimized the set of molecules at B3LYP/6-31G level of theory, and a single point energy calculation is done at B3LYP/6-311+G(d,p) level of theory for the reactants (depicted in Fig. 1) and the corresponding deprotonated molecule. In the calculation, we considered all the reactant as neutral, with a multiplicity one. Similarly, for the product, the deprotonated molecule, is associated with charge –1, and multiplicity one. The energies of the reactant and product at B3LYP/6-311+G(d,p) level of theory are reported in Table 1, columns 2 and 3, and the reaction energies (in kcal/mol) are reported in column 4. The first and the second columns of Table 1 reports the single point energies for the benchmark molecules {I-IV} with conjugated double bonds, {V-VII} with isolated covalent double bonds, and {VIII-X} with both single and double bonds.

For benchmarking our model, we have followed a similar scheme with the same scale factor (*g*) and rotation angles, as depicted in Fig. 1 for model system preparation. In each of these reactions, the model system is constructed around the organic functional group, by scissoring the double bond. All the ONIOM calculation reported in Table 1 is performed with the same combination of the scale factor (*g*) and rotation angle. The final column in Table 1 report the difference in ONIOM and FC reaction energies $\left(\delta E_{\text{Reaction}}^{\text{Error}}\right)$. The conjugated molecules (I-III) shows larger deviation in reaction energy compared to the isolated double bonds. Also, the benchmark studies show that the scaling factor, *g* for the conjugated molecule must be lower in magnitude than the isolated double-bonded systems. However, a fair agreement of the ONIOM dissociation energy with FC validates the treatment of the model system boundary through a two-link-atom ONIOM model-system preparation step.

(2) Comparison of forces and geometrical parameters of the molecules

For benchmarking and verifying the accuracy of the two-link-atom ONIOM model system preparation method, we have evaluated the atomic forces and performed a geometry optimization. A set of benchmark molecules depicted in Fig. 2

Table 1. Comparison of the full calculation (FC) at B3LYP/6-311+G(d,p) and ONIOM (B3LYP/6-311+G(d,p): HF/3-21G) reactant, product energies (in a.u.), reaction energies and error in reaction energies (in kcal/mol) of the molecules depicted in Fig. 2. See text for details

Molecule	$E^{FC}_{Reactant}$	$E^{FC}_{Product}$	$\Delta E^{FC}_{Reaction}$	$\Delta E^{ONIOM}_{Reaction}$	$\delta E^{Error}_{Reaction}$
			(kcal/mol)	(kcal/mol)	(kcal/mol)
I	–426.68881	–426.09030	375.57	376.89	1.33
II	–749.66419	–749.10577	350.41	351.96	1.54
III	–406.81725	–406.19132	392.78	394.18	1.40
IV	–424.55164	–423.99669	348.23	348.93	0.69
V	–350.48457	–349.87802	380.62	382.04	1.43
VI	–330.61078	–329.96639	404.36	405.44	1.08
VII	–673.45769	–672.89028	356.05	356.27	0.22
VIII	–1170.2101	–1169.60790	377.87	377.42	0.44
IX	–1493.1803	–1492.61610	354.04	354.31	0.26
X	–1150.33423	–1149.69717	399.76	400.43	0.67

with conjugated and isolated double bonds are considered, on which the ONIOM boundary effects are highly visible. The molecule number is kept the same in Fig. 2, Table 1, and Table 2. We report an illustrative example of the geometrical parameters of some benchmark molecules depicted in Fig. 2. The geometrical parameters reported in Table 2 are explicitly depicted in Fig. 2. As an illustrative benchmark, we have taken molecules I, II, III, IV, and V depicted in Fig. 2, where the ONIOM results are more visible. The size of the model system is kept similar for all I, II, IV, and V molecules in the geometry optimization cycles. Also, the initial definition and size of the model system are kept constant during optimization cycles. After the geometry optimization, the root means square (RMS) of forces show close agreement, and the corresponding FC and ONIOM geometrical parameters corroborate within 0.001 Å. A comparison of benchmark molecules reported in Table 2 shows that the geometrical parameters of the model system, Region I is close to the high-level, and ones in the Region II are close to the low-level calculations, respectively.

The geometrical parameters (in Å) reported in Table 2 show a fair agreement with FC and the error is typically less than 0.001 Å. The boundary region geometrical parameters show a larger deviation compared to the one buried deep inside the model system. What is remarkable is the possibility of estimating the FC geometrical parameters through the two-link-atom ONIOM model system preparation. The agree-

Table 2. Comparison of optimized geometrical parameters (distance in Å) of molecules I, II, III, IV, and V depicted in Fig. 1. The full calculation (FC) is performed at B3LYP/6-311+G(d,p) and ONIOM at B3LYP/6-311+G(d,p): HF/6-31G(d). FC geometrical parameters are reported outside and ONIOM inside the brackets, respectively. See Fig. 2 for the description of the geometrical parameter and text for details

Geometrical	Molecules				
parameters	I	II	III	IV	V
R_1	1.436 (1.435)	1.867 (1.866)	1.474 (1.474)	1.358 (1.358)	1.429 (1.430)
R_2	1.098 (1.098)	1.092 (1.092)	1.096 (1.096)	1.204 (1.205)	1.099 (1.098)
R_3	1.493 (1.494)	1.491 (1.492)	1.504 (1.504)	1.515 (1.515)	1.527 (1.527)
R_4	1.088 (1.088)	1.088 (1.088)	1.090 (1.090)	1.093 (1.099)	1.097 (1.093)
R_5	1.343 (1.341)	1.345 (1.344)	1.345 (1.345)	1.502 (1.504)	1.503 (1.506)
R_6	1.089 (1.089)	1.089 (1.089)	1.090 (1.090)	1.087 (1.085)	1.091 (1.089)
R_7	1.446 (1.455)	1.445 (1.440)	1.447 (1.447)		
R_8	1.089 (1.086)	1.089 (1.088)	1.089 (1.089)		

ment of the geometries with the FC shows that the method is adaptable for any fragment-based method, that involves the construction of subsystem or model system preparations step.

Concluding remarks

In this work, we have proposed a 'two-link-atom' ONIOM model system preparation to treat the boundary with covalent double bonds. In this method, two-H-link-atom centers are treated as an electron buffer region. This new way of substituting two-link-atom is independent of any arbitrary definition of atoms involved, is defined based on saturating the double valency and is independent of the level of theory and basis set employed. Our method is benchmarked for exploring reaction energies on systems with multiple-link atoms. We have benchmarked the method on ten reactions, involving conjugated and isolated double-bonds. The method is demonstrated for an accurate estimation of reaction energies, the difference vis-à-vis its FC counterparts is observed to be within an accuracy of 1.0 kcal/mol. The performance of the method seems more impressive while estimating the forces and the geometrical parameters of large molecules. The conjugated molecule shows better agreement with a lower magnitude of the chosen scaling factor when compared with the isolated double bonds. This confirms that the accuracy of the two-link-atom ONIOM method can be improved further by appropriately choosing the scaling factor (g) and the rotational angle $R(\theta)$ of the link H-atom. Considering the high accuracy, and the need for minimal hardware and economy in computation time, we trust that our method would be valuable for studying the structure and energetics of large molecules. The present method opens a way for exploring the higher energy derivatives and related molecular properties of systems having isolated or conjugated double bonds.

Acknowledgements

JJ is thankful to the University Grants Commission (UGC), Govt. of India for the startup grant. SM thank University of Hyderabad and UGC for non-NET fellowship. Authors are thankful to the Center for Modelling and Simulations Designing (CMSD), University of Hyderabad for providing the computational facility.

References

1. "Fragmentation: Toward Accurate Calculations on Complex Molecular Systems", ed. Mark S. Gordon, John Wiley & Sons Inc., Chichester, UK, Hoboken, NJ, 2017, pp. 141-163.
2. M. S. Gordon and L. V. Slipchenko, *Chem. Rev.*, 2015, **115**, 5605.
3. N. Sahu and S. R. Gadre, *Acc. Chem. Res.*, 2014, **47**, 2739.
4. K. Raghavachari and A. Saha, *Chem. Rev.*, 2015, **115**, 5643.
5. L. A. Curtiss, P. C. Redfern and K. Raghavachari, *J. Chem. Phys.*, 2007, **126**, 084108.
6. N. J. DeYonker, T. R. Cundari and A. K. Wilson, *J. Chem. Phys.*, 2006, **124**, 114104.
7. A. D. Boese, M. Oren, O. Atasoylu, J. M. L. Martin, M. Kallay and J. Gauss, *J. Chem. Phys.*, 2004, **120**, 4129.
8. J. W. Ochterski, G. A. Petersson and J. A. Montgomery (Jr.), *J. Chem. Phys.*, 1996, **104**, 2598.
9. A. Karton, E. Rabinovich and J. M. Martin, *J. Chem. Phys.*, 2006, **125**, 144108.
10. A. Tajti, P. Szalay, A. Csaszar, M. Kallay, J. Gauss, E. Valeev, B. Flowers, J. Vazquez and J. Stanton, *J. Chem. Phys.*, 2004, **121**, 11599.
11. A. Warshel and M. Levitt, *J. Mol. Biol.*, 1976, **103**, 227.
12. U. C. Singh and P. A. Kollman, *J. Comp. Chem.*, 1986, **7**, 718.
13. M. J. Field, P. A. Bash and A. M. Karplus, *J. Comp. Chem.*, 1990, **11**, 700.
14. J. Aqvist and A. Warshel, *Chem. Rev.*, 1993, **93**, 2523.
15. F. Maseras and K. Morokuma, *J. Comp. Chem.*, 1995, **16**, 1170.
16. T. Mordasini and W. Thiel, "Combined Quantum Mechanical and Molecular Mechanical Approaches Chimia", 1998, **52**, 288.
17. G. Monard and K. M. Merz, *Acc. Chem. Res.*, 1999, **32**, 904.
18. J. L. Gao and D. G. Truhlar, *Ann. Rev. Phys. Chem.*, 2002, **53**, 467.
19. L. W. Chung, W. M. C. Sameera, R. Ramozzi, A. J. Page, M. Hatanaka, G. P. Petrova, T. V. Harris, X. Li, Z. Ke, F. Liu, H. Li, L. Ding and K. Morokuma, *Chem. Rev.*, 2015, **115**, 5678.
20. S. Humbel, S. Sieber and K. Morokuma, *J. Chem. Phys.*, 1996, **105**, 1959.
21. M. Svensson, S. Humbel, R. Froese, T. Matsubara, S. Sieber and K. Morokuma, *J. Phys. Chem.*, 1996, **100**, 19357.
22. P. B. Karadakov and K. Morokuma, *Chem. Phys. Lett.*, 2000, **317**, 589.
23. T. Vreven and K. Morokuma, *J. Comp. Chem.*, 2000, **21**, 1419.
24. T. Vreven, B. Mennucci, C. da Silva, K. Morokuma and J. Tomasi, *J. Chem. Phys.*, 2001, **115**, 62.
25. T. Vreven and K. Morokuma, *Theor. Chem. Acc.*, 2003, **109**, 125.

26. W. Yang and T. Lee, *J. Chem. Phys.*, 1995, **103**, 5674.
27. Y. Zhang and H. Lin, *J. Chem. Theor. Comp.*, 2008, **4**, 414.
28. S. L. Dixon and K. M. Merz, *J. Chem. Phys.*, 1996, **104**, 6643.
29. V. Gogonea, L. M. Westerhoff and K. M. Merz, *J. Chem. Phys.*, 2000, **113**, 5604.
30. N. J. Mayhall and K. Raghavachari, *J. Chem. Theory Comput.,* 2010, **6**, 3131.
31. K. V. Jovan Jose and K. Raghavachari, *J. Chem. Theory Comput.,* 2014, **10**, 4351.
32. J. L. Gao, P. Amara, C. Alhambra and M. J. Field, *J. Phys. Chem. A*, 1998, **102**, 4714.
33. J. Z. Pu, J. L. Gao and D. G. Truhlar, *Chem. Phys. Chem.*, 2005, **6**, 1853.
34. S. D. Yeole and S. R. Gadre, *J. Chem. Phys.*, 2010, **132**, 094102.
35. S. Dapprich, I. Komaromi, K. S. Byun, K. Morokuma and M. J. Frisch, *J. Mol. Struct.: THEOCHEM*, 1999, **461**, 1.
36. Gaussian 09, Revision D.01, M. J. Frisch, G. W. Trucks, H. B. Schlegel, G. E. Scuseria, M. A. Robb, J. R. Cheeseman, G. Scalmani, V. Barone, B. Mennucci, G. A. Petersson, H. Nakatsuji, M. Caricato, X. Li, H. P. Hratchian, A. F. Izmaylov, J. Bloino, G. Zheng, J. L. Sonnenberg, M. Hada, M. Ehara, K. Toyota, R. Fukuda, J. Hasegawa, M. Ishida, T. Nakajima, Y. Honda, O. Kitao, H. Nakai, T. Vreven, J. A. Montgomery (Jr.), J. E. Peralta, F. Ogliaro, M. Bearpark, J. J. Heyd, E. Brothers, K. N. Kudin, V. N. Staroverov, R. Kobayashi, J. Normand, K. Raghavachari, A. Rendell, J. C. Burant, S. S. Iyengar, J. Tomasi, M. Cossi, N. Rega, N. J. Millam, M. Klene, J. E. Knox, J. B. Cross, V. Bakken, C. Adamo, J. Jaramillo, R. Gomperts, R. E. Stratmann, O. Yazyev, A. J. Austin, R. Cammi, C. Pomelli, J. W. Ochterski, R. L. Martin, K. Morokuma, V. G. Zakrzewski, G. A. Voth, P. Salvador, J. J. Dannenberg, S. Dapprich, A. D. Daniels, Ö. Farkas, J. B. Foresman, J. V. Ortiz, J. Cioslowski and D. J. Fox, Gaussian, Inc., Wallingford CT, 2009.